

Restriction Landmark Genomic Scanning of Mouse Liver Tumors for Gene Amplification: Overexpression of Cyclin A2

Ramsi Haddad,¹ Arlene D. Morrow, Christoph Plass,² and William A. Held³

Department of Molecular and Cellular Biology, Roswell Park Cancer Institute, Buffalo, New York 14263

Received June 15, 2000

SV40 T/t antigen-induced liver tumors from transgenic mice were analyzed by Restriction Landmark Genomic Scanning (RLGS). Using *NotI* as the restriction landmark, RLGS targets CpG islands found in gene-rich regions of the genome. Since many RLGS landmarks are mapped, the candidate gene approach can be used to help determine which genes are altered in tumors. RLGS analysis revealed one tumor-specific amplification mapping close to *CcnA2* (cyclin A2) and *Fgf2* (fibroblast growth factor 2). Southern analysis confirmed that both oncogenes are amplified in this tumor and in a second, independent liver tumor. Whereas *Fgf2* RNA is undetectable in tumors, *CcnA2* RNA and cyclin A2 protein was overexpressed in 25 and 50% of tumors, respectively. Combining RLGS with the candidate gene approach indicates that cyclin A2 amplification and overexpression is a likely selected event in transgenic mouse liver tumors. Our results also indicate that our mouse model for liver tumorigenesis in mice accurately recapitulates events observed in human hepatocellular carcinoma. © 2000

Academic Press

Key Words: restriction landmark genomic scanning; transgenic mice; liver tumorigenesis; cell cycle; DNA amplification.

A transgenic mouse model of hepatocellular carcinoma (HCC) has been utilized to identify genetic and epigenetic alterations associated with tumor progression (1–6). Transgenic mouse line MTD2BL/6 uses the major urinary protein (MUP) promoter to drive SV40 T/t Antigen (TAg) expression almost exclusively in the adult liver (3). Transgene expression is activated at

puberty in male mice at approximately 3 weeks of age and remains activated (3). This results in progressive dysplasia and apoptosis of the original hepatocyte population which continues, reaching maximal levels at about 8–10 weeks of age. At about this time, multiple foci of small cells are first observed that continue growing to confluence, completely replacing the liver parenchyma by about 16 weeks of age (7). The continued growth of these small cells results in liver hyperplasia. Neoplastic nodules develop on this hyperplastic background and grow into encapsulated tumors (7) which undergo angiogenesis (3), may become locally invasive, and have been observed, although rarely, to metastasize to the lung.

Restriction Landmark Genomic Scanning (RLGS) effectively detects tumor-specific alterations including changes in DNA methylation, DNA loss and DNA amplification. RLGS is a method for the two-dimensional display of end-labeled genomic DNA restriction enzyme fragments that can resolve 1500 to 2000 genomic restriction landmarks in a single gel (8, 9). When using the methylation sensitive endonuclease *NotI* as the restriction landmark, the analyzed sequences are primarily those associated with CpG islands which are found in gene rich regions of the genome (6, 8, 9). Genetic loss or DNA amplification in tumors is observable as a decreased or increased intensity of these sequences (spots) on an RLGS gel.

RLGS has been applied to the genetic analysis of both human and mouse tumors (5, 6, 10–12). RLGS and spot cloning has revealed amplifications in the *CDK6* gene in human gliomas (12) and the *CTSB* gene (cathepsin B) in human esophageal adenocarcinoma (11). Analysis of mouse liver tumors indicated alterations in the methylation patterns of genes thought to be involved in tumorigenesis, *p16^{Ink4a}* and $\alpha 4$ integrin (6), Insulin-like growth factor binding protein-7 (13), as well as within unknown genetic sequences (5, 6).

RLGS was applied to MTD2BL/6 liver tumors to further define the genetic events involved in liver tu-

¹ Present address: Van Andel Institute, 201 Monroe Avenue NW, Grand Rapids, MI 49503.

² Division of Human Cancer Genetics, Ohio State University, 420 West 11th Avenue, Columbus, OH 43210.

³ To whom correspondence should be addressed. Fax: (716) 845-8169. E-mail: wheld@mcbio.med.buffalo.edu.

morigenesis. Many RLGS spots are mapped (14) enabling the use of the candidate gene approach to help identify genes that are altered in tumors. Such an approach bypasses the rate-limiting step of spot cloning for gene identification.

Our RLGS analysis revealed one tumor with a discrete amplification event that mapped close to two known oncogenes, *Fgf2* (fibroblast growth factor 2) and *CcnA2* (cyclin A2). Since genetic amplification is a characteristically selective event during tumorigenesis, we examined the copy number and expression patterns of genes within this chromosomal region in a panel of MTD2BL/6 liver tumors. Thus, RLGS provided a target region for investigation and subsequent analysis indicates that *CcnA2*, a gene within this target region, is frequently overexpressed regardless of whether it was amplified or not.

MATERIALS AND METHODS

MTD2BL/6 is a congenic line of MTD2 (1–6) back-crossed to C57BL/6Ros for more than 20 generations. Tumors were dissected as described (4).

RLGS DNA isolation and RLGS were performed using *NotI*–*PstI*–*PvuII* (8).

Southern and Northern analysis was performed as described (2, 4).

The following IMAGE Consortium clones (Research Genetics) were sequenced for verification and used as probes with the IMAGE clone identification number in parentheses: *Evi1* (1055020), *CcnA2* (735378), *AnxV* (678904) and *Il2* (722885). The SV40 Tag probe is a 2.7 kb *EcoRI*–*XbaI* fragment from plasmid p11AsT (3). The histone *H3-2* probe is a 0.6 kb *PvuII* fragment from plasmid pGH3 (kindly provided by C. Rogler).

Protein was prepared from tissue using TRIzol Reagent (Life Technologies) and measured with the Bio-Rad DC protein assay (Bio-Rad). Thirty μ g protein was transferred onto Immobilon-P PVDF membranes (Millipore) after SDS–PAGE (15, 16). The following rabbit polyclonal antibodies were used for detection: cyclin A2 (C19) and cyclin D1 (M-20) (Santa Cruz Biotechnology). Horseradish peroxidase-conjugated antibody (Santa Cruz Biotechnology) was used as the secondary antibody followed by enhanced chemiluminescence (Amersham) for detection.

The genetic distance between *Evi1* and *CcnA2* was determined using the Copeland-Jenkins (C57BL/6 \times M. spretus)F1 \times C57BL/6 back-cross mapping panel in the Mouse Genome Database (17) and calculated by inferring the genotype of untyped and nonrecombinant individuals using Map Manager v.2.6.3 (18).

For RT-PCR, cDNA was produced by the Superscript Preamplification System (Life Technologies) using 5 μ g of total RNA. PCRs were as described (4). *Fgf2* was amplified using a forward primer of 5'-gcatcactcgcttc-3' and a reverse primer of 5'-agtatggcctctgtc-3' with an annealing at of 55°C (19). *CcnA2* was amplified as described (19).

RESULTS

Liver Tumor 742/2-1 Has an Amplification Which Maps Close to CcnA2 and Fgf2

RLGS was performed on liver tumors generated in MTD2BL/6 transgenic mice using the enzyme combination *NotI*–*PstI*–*PvuII* (8). MTD2BL/6 is a congenic mouse line of the MTD2 MUP-Tag transgene (3) on a C57BL/6J genetic background. *NotI* was chosen as the

restriction landmark because these restriction sites appear principally in CpG islands which are associated with gene rich regions of the genome. Thus, altered spots on an RLGS gel are more likely to be directly linked to genes. Furthermore, 106 C57BL/6J-specific spots have been mapped in B \times D recombinant inbred strains with the enzyme combination *NotI*–*PstI*–*PvuII* (14). Consequently, RLGS spot alterations in our analysis could be localized to specific chromosomal regions and permit the application of the candidate gene approach.

RLGS analysis was performed on genomic DNA extracted from 14 liver tumors. Liver tumor 742/2-1 had 6 spots amplified approximately 50-fold over control tissue, three of which are shown (Fig. 1). Since all 6 spots are equally amplified, this suggests that they are part of the same contiguous amplicon. Two of the amplified spots, spots B77 (locus *D3Rik65*) and B24 (locus *D3Rik66*), have previously been mapped to proximal chromosome 3 close to *CcnA2* (cyclin A2) and *Fgf2* (fibroblast growth factor 2) (14, 17). Both are genes that have been implicated in tumorigenesis and represent candidate genes driving selection for the amplification.

The Amplicon in Tumor 742/2-1 and a Second, Independent Liver Tumor, May Be as Small as 0.27 cM and Includes CcnA2 and Fgf2

Southern blot analysis was used to determine which genes are amplified and the approximate length of the amplicon found in liver tumor 742/2-1. A simplified consensus genetic map of proximal chromosome 3 is shown (Fig. 2A) (17). Within 5 cM of *D3Rik65,66* are three known oncogenes: *Evi1* (endogenous viral integration site 1), *CcnA2* (cyclin A2) and *Fgf2* (fibroblast growth factor 2). *Evi1* is a zinc-finger protein that has been implicated in the leukemic transformation in a mouse model of tumorigenesis (20). *CcnA2* has been implicated in human HCC tumorigenesis (21–23). *Fgf2* is an endothelial growth factor that can induce tumor angiogenesis (24) and has been implicated in the progression of several human tumor types (25, 26). In addition, loci *D3Rik65, 66* are close to *Il2* and *Id3*, loci for which a high resolution genetic map has been generated (27) and is also shown (Fig. 2B).

Southern hybridizations of DNA extracted from control and liver tumor tissues were performed using probes specific to *Evi1*, *AnxV*, *CcnA2*, *Fgf2* and *Il2* (Fig. 2C). *AnxV*, *CcnA2* and *Fgf2* are clearly amplified in liver tumor 742/2-1 relative to control tissues and other liver tumors (Fig. 2C). The amplification is estimated to be about 50-fold, consistent with the level of amplification observed in the RLGS gel (Fig. 1). Since *Evi1* is not amplified (Fig. 2C), it can be excluded as a candidate oncogene driving selection for the amplification.

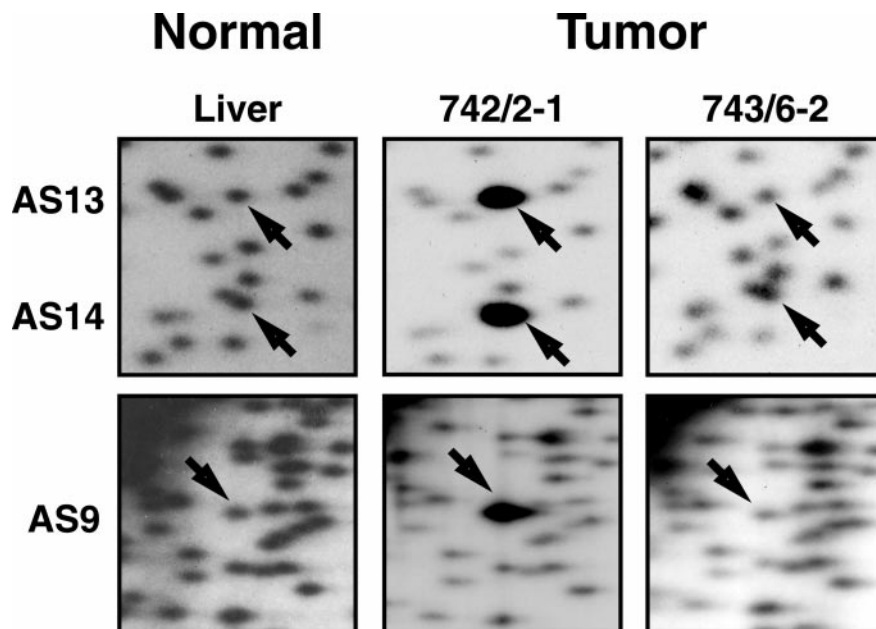


FIG. 1. RLGS gel enlargements displaying representative spot amplification in tumor 742/2-1. RLGS was performed on normal liver (normal) and 14 MTD2BL/6 liver tumors of which tumors 742/2-1 and 743/6-2 are shown (tumor). Only portions of the RLGS profiles are shown. Three of six amplified spots (AS1, AS2, and AS3) in tumor 742/2-1 are shown. AS3 corresponds to spot B24 (locus *D3Rik66*) and has been mapped close to *CcnA2* and *Fgf2* (14).

Thus, the proximal breakpoint for the amplicon lies between *Evi1* and *AnxV*. *Il2* is not amplified (Fig. 2C) which indicates that the distal breakpoint of the amplicon lies between *Fgf2* and *Il2*. Since the physical distance between *Fgf2* and *Il2* is known to be approximately 350 kb (27), this amplification breakpoint is well defined. Since the genetic distance between *Evi1* and *AnxV* is 6.5 cM (17) and the physical distance between these two genes has not been defined, the proximal amplification breakpoint is ill defined. Thus, the minimal size of the amplicon is 0.27 cM and suggests that *CcnA2*, *Fgf2*, or an unknown oncogene drives selection for this amplification.

To further investigate the amplification of this chromosomal region during liver tumorigenesis, a panel of 18 MTD2BL/6 liver tumors was analyzed using Southern blotting (Fig. 2D). Southern hybridizations of DNA extracted from control and liver tumor tissues were performed using probes specific to *Evi1*, *AnxV*, *CcnA2*, *Fgf2* and *Il2* (Fig. 2D). It is clear that similar to tumor 742/2-1, tumor 742/3-2 has an amplicon which includes *AnxV*, *CcnA2* and *Fgf2* (Fig. 2D). The magnitude of this second amplicon is slightly less and estimated to be approximately 30 fold. The two amplicons appear to be of similar length insofar as the same genes are amplified in both tumors.

Combined with the 14 MTD2BL/6 liver tumors analyzed by RLGS, 2/32 liver tumors show amplification of this region of chromosome 3 (Table 1). Thus, amplification of this region occurs with a frequency of about 6%.

CcnA2 RNA Is Up-Regulated in Liver Tumors, Whereas *Fgf2* RNA Is Low or Undetectable in Liver Tumors

If either *CcnA2* or *Fgf2* were driving selection for the amplicon in either tumor 742/2-1 or tumor 742/3-2, one would expect to see increased levels of the selective transcript within the tumor. Furthermore, the observed amplicon may represent a selective advantage in MTD2BL/6 liver tumors that can be brought about through mechanisms of overexpression other than DNA amplification. We therefore analyzed the same panel of 18 MTD2BL/6 liver tumor RNAs for expression of *CcnA2* and *Fgf2*.

A representative Northern hybridization of total RNA extracted from control tissues and liver tumors is shown using a probe specific to *CcnA2* (Fig. 3A). Ethidium bromide staining of the gel indicates equal loading of RNA in almost all lanes (Fig. 3A). Normal adult liver and kidney RNA served as negative controls since these tissues are not actively cycling. Since MTD2BL/6 liver tumors arise in hyperplastic liver (7), a developmental series of transgenic liver RNA was included to trace the preneoplastic expression patterns of MTD2BL/6 liver leading up to liver neoplasia.

CcnA2 RNA is easily detected in subconfluent NIH 3T3 cells (Fig. 3A, lane a). As expected for an actively cycling tissue, *CcnA2* expression is detectable in 1 week liver (Fig. 3A). *CcnA2* expression is undetectable in 5 week transgenic liver (Fig. 3A). This is consistent

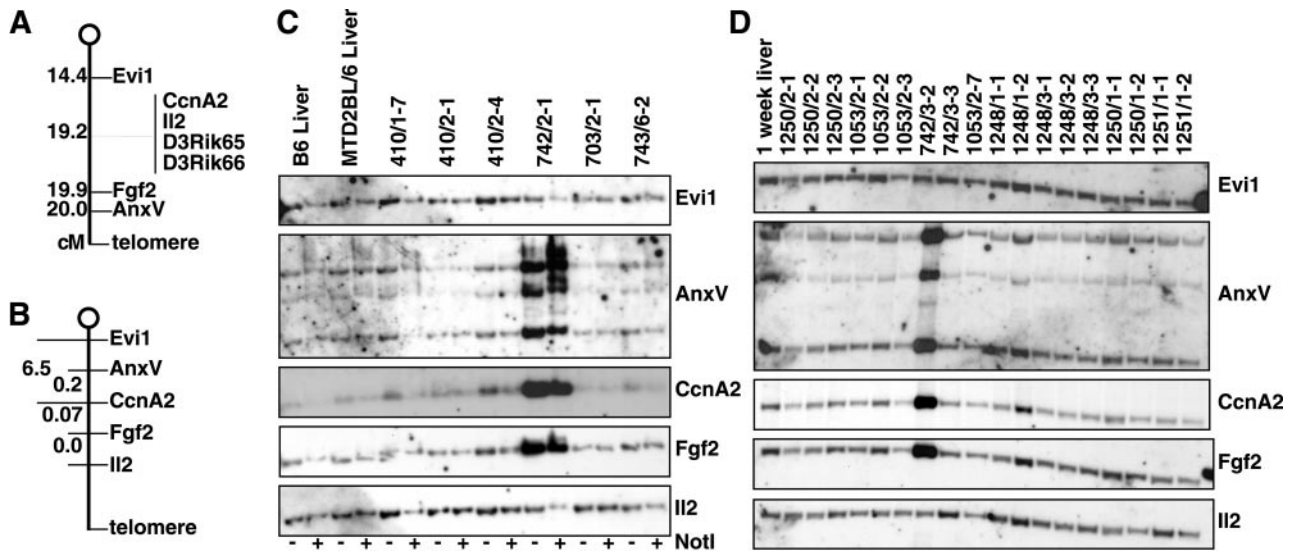


FIG. 2. The amplicons in tumor 742/2-1 and 742/3-2 include *CcnA2* and *Fgf2*. (A) Schematic genetic map of proximal chromosome 3. The depiction is not to scale. Numbers indicate genetic distance of loci from the centromere and are based on the 1998 Chromosome 3 consensus map from the Mouse Genome Database (17). *D3Rik65* and *D3Rik66* correspond to spots B77 (data not shown) and B24 (14). (B) High-resolution genetic map of the chromosome 3 region surrounding *CcnA2* and *Fgf2*. The depiction is not to scale. Numbers indicate the genetic distance in centimorgans between loci. The genetic distance between *Evi1* and *CcnA2* is based on the Copeland-Jenkins (C57BL/6 × *M. spretus*)F1 × C57BL/6 back-cross (refer to Materials and Methods) (17). All other genetic distances are taken from Denny *et al.* (27). (C) Southern analysis of tumor 742/2-1 indicates the amplicon includes *AnxV*, *CcnA2* and *Fgf2*. Ten μ g of total liver tumor DNA or control DNA was digested with *PvuII* in the presence (+) or absence (−) of *NotI* as indicated and separated on a 1% agarose gel. After transfer onto nylon membrane, the blot was sequentially hybridized with probes specific for *Evi1*, *AnxV*, *CcnA2*, *Fgf2* and *Il2* as indicated. (D) Southern analysis of tumor 742/3-2 indicates the amplicon includes *AnxV*, *CcnA2* and *Fgf2*. Note that tumor 742/3-3 from the same animal does not have an amplification of this region. Ten micrograms of total liver tumor DNA or control DNA was digested with *PstI* and probed as indicated above.

with the fact that livers in normal mice of this age are essentially fully grown and that MTD2BL/6 transgenic mice are just beginning to express TAG at this time. *CcnA2* expression is high in 8 week transgenic liver and remains high in 15 week transgenic liver (Fig. 3A). At this age (15 weeks), transgenic livers are hyperplastic but there are no definitive tumor nodules. Liver tumors begin to arise in this hyperplastic background in these animals shortly after 15 weeks of age (7). As well, the RLGS profile of 15 week hyperplastic liver is essentially identical to normal liver (Held, unpublished results). Thus, the *CcnA2* expression levels in tumors were compared to those observed in hyperplastic, pre-neoplastic, 15 week livers from transgenic mice.

Consistent with the amplification of the *CcnA2* gene in tumor 742/3-2, exceptionally high *CcnA2* RNA levels are expressed (Fig. 3A). (Unfortunately, tumor sample 742/2-1 was exhausted and expression levels of *CcnA2* could not be measured.) Tumors 1250/2-3 and 1053/2-2 also express *CcnA2* RNA to levels above those observed in 15 week hyperplastic liver (Fig. 3A). In the 18 liver tumors analyzed for *CcnA2* RNA expression, 4/18 tumors expressed *CcnA2* RNA to levels at least 4-fold higher than levels observed in 15 week liver (Table 1). As well, 6/18 tumors expressed *CcnA2* RNA to levels equal to or up to 3-fold as high as 15 week hyperplastic liver. Thus, *CcnA2* RNA is highly overexpressed in approximately 25% of MTD2BL/6 liver tumors. These

RNA expression results also indicate that *CcnA2* overexpression in liver tumors is not a generalized phenomenon of MTD2BL/6 liver tumorigenesis and is consistent with overexpression occurring in a subset of liver tumors.

Fgf2 expression in tumors was measured using RT-PCR. Control RT-PCRs with *CcnA2*-specific primers gave expression levels similar to those observed with the *CcnA2* Northern analysis (data not shown). The *Fgf2* primers generated a 424 base pair PCR product (19) and a nonspecific, diffuse band that appears below 400 bp in almost all lanes (Fig. 3B). Clearly, the specific *Fgf2* PCR product is detectable in RNA extracted from control NIH-3T3 cells, control liver, and in RNA extracted from early, preneoplastic stages of liver tumor progression, especially at 8 and 15 weeks (Fig. 3B). Tumor samples do not express detectable *Fgf2* indicating that *Fgf2* expression is not common in the MTD2BL/6 liver tumor model. Indeed, despite the fact that the *Fgf2* gene is amplified approximately 30-fold in tumor 742/3-2 (Fig. 2C), no *Fgf2* expression is detectable. This result indicates that *Fgf2* may be excluded as the gene driving selection for the amplification on the proximal region of chromosome 3.

The MTD2BL/6 transgenic line uses TAG as the activating oncogene which drives liver tumorigenesis. Since it has been suggested that TAG is able to transactivate *CcnA2* RNA expression in rat F111 cells (28),

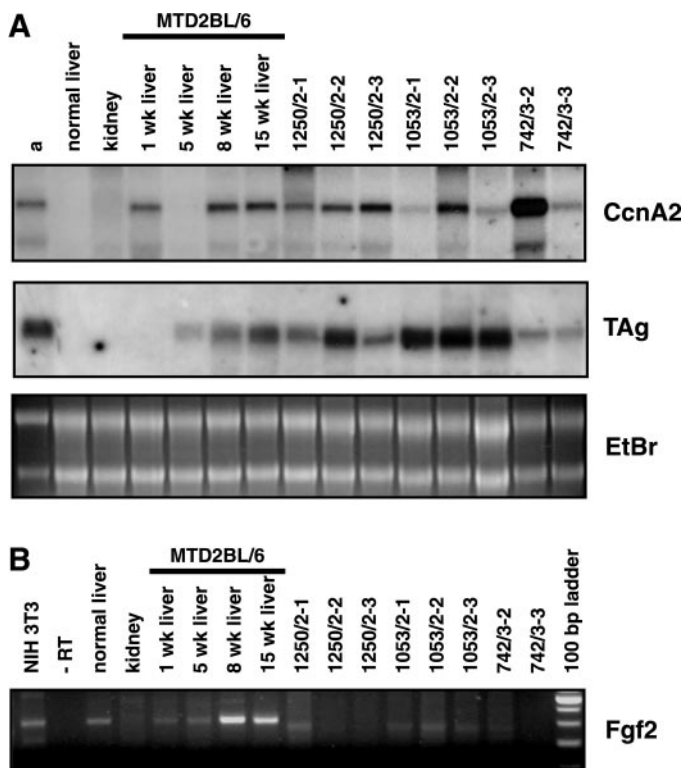


FIG. 3. *CcnA2* overexpression occurs in liver tumors, whereas *Fgf2* is not detectable in tumors. (A) Representative Northern blots of *CcnA2* and T-Antigen expression. Twenty micrograms of total control tissue or liver tumor RNA were separated on 1.7% agarose gels (with the exception of lane a in the *CcnA2* panel which contains 10 μ g of RNA). Ethidium bromide-stained gels indicate that there was equal loading of RNA in almost all lanes (EtBr panel). The ethidium bromide-stained RNA shown corresponds to the *CcnA2* Northern blot. After transfer onto nylon membranes, the blots were hybridized with probes specific to *CcnA2* and T-Antigen. Lane (a) is RNA extracted from NIH-3T3 cells on the *CcnA2* Northern blot and tumor 1053/2-7 on the TAG Northern blot. (B) Representative RT-PCR of *Fgf2*. Five μ g of total RNA was reverse transcribed and was subsequently PCR amplified in separate reactions using primers specific to *Fgf2* (refer to Materials and Methods for primer sequence). The *Fgf2* primer pair results in an amplification product of 425 base pairs (19). The intense band in the 100-bp ladder represents 600 bp and DNA fragments below this band are 500, 400 and 300 bp, respectively.

TAg RNA levels were measured to exclude the possibility that *CcnA2* RNA overexpression in some tumors was the result of high TAg expression. As expected, TAg is undetectable in Northern hybridizations of RNA extracted from normal mouse liver and kidney (Fig. 3A). Even though tumor samples express variable levels of TAg, no correlation is evident with respect to TAg expression and *CcnA2* expression at the RNA level. For instance, liver tumor sample 1053/2-3 has high TAg RNA levels without high levels of *CcnA2* RNA (Fig. 3A). As well, tumor 742/3-2 has very high *CcnA2* RNA levels, but low TAg RNA levels (Fig. 3A).

These expression studies suggest that *CcnA2* expression is a selective event during MTD2BL/6 liver tumor-

igenesis and not driven by TAg expression. These results further indicate that *Fgf2* expression is unlikely to be the gene driving selection for the amplification observed in tumor 742/3-2.

Cyclin A2 Protein Levels Are Far in Excess of Levels Required for Active Growth and Do Not Always Correlate with a High Proportion of Cells in S-Phase

Since cyclin A2 protein expression is controlled at both transcriptional and post-transcriptional levels (29), cyclin A2 protein was measured using immunoblotting. Figure 4A is a representative Western blot performed with protein extracts prepared from the same tissue samples used to prepare total RNA. Coomassie brilliant blue stained gels indicate equal loading of proteins in all lanes (data not shown). Normal adult liver tissue does not have detectable cyclin A2 (Fig. 4A). In the developmental liver series, 1 week liver has high levels of cyclin A2 (Fig. 4A). Cyclin A2 levels are barely detectable in 5 week liver and increase in 8 week and 15 week MTD2BL/6 liver (Fig. 4A). This pattern of expression is consistent with the RNA results (Fig. 3A).

Since 15 week hyperplastic liver is the tissue from which tumors develop, it is appropriate to compare cyclin A2 protein levels with 15 week transgenic liver. In tumor samples, cyclin A2 is present at very high levels in many tumors (Fig. 4A). For instance, the levels of cyclin A2 in tumors 1053/2-2,-3 and 742/3-2,-3 are much higher than levels observed in 15 week transgenic liver (Fig. 4A). That is, cyclin A2 protein levels in some tumors are much higher than levels observed in a tissue undergoing active growth. Interestingly, tumor 742/3-2 is amplified at the *CcnA2* locus and expresses cyclin A2 levels similar to 1053/2-3 which is not (Fig. 4A). Thus, cyclin A2 overexpression in some tumors does not require DNA amplification. The analysis demonstrated that 9/18 liver tumors overexpress cyclin A2 protein at least 4 fold over levels observed in 15 week liver (Fig. 4A, Table 1). Therefore, cyclin A2 protein is frequently expressed at levels far in excess of those observed in actively growing tissue.

TABLE 1

Summary of Cyclin Overexpression and Amplification in MTD2BL/6 Liver Tumors Analyzed

	DNA	RNA	Protein ^a
Liver tumors with cyclin A2 overexpression or amplification	2/34	4/18	9/18
Liver tumors with cyclin D1 overexpression or amplification	ND	ND	6/18

^a Overexpression indicates RNA or Protein expression levels at least 4 fold above 15 week hyperplastic liver. ND, not determined.

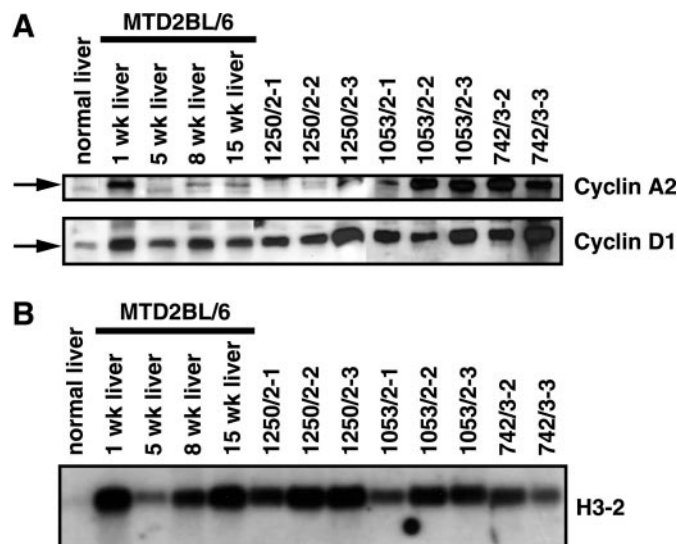


FIG. 4. Cyclin A2 protein is overexpressed in tumors. (A) Representative Western analysis of Cyclin A2 and Cyclin D1 protein expression. Thirty micrograms of protein was separated on a 12% polyacrylamide gel in the presence of 0.1% SDS. Coomassie brilliant blue-stained gels indicate equal loading of proteins in all lanes (data not shown). After transfer to PVDF membrane, protein was blotted with antibody specific to cyclin A2 and cyclin D1 using chemiluminescence as the method of detection. (B) Representative Northern analysis of histone *H3-2*. Histone *H3-2* is expressed exclusively in S-phase cells (32). Ten micrograms of RNA was separated on a 1.7% agarose gel. Ethidium bromide staining prior to transfer onto nylon membrane indicates that there was equal loading of RNA in all lanes (data not shown). After transfer onto nylon membrane, the blot was hybridized with a probe specific to histone *H3-2*.

To verify that cyclin A2 protein overexpression is not the consequence of a general overexpression of cyclins in some tumors, cyclin D1 protein was measured because it is the major G1-phase specific cyclin (29, 30). While 1 week transgenic liver has high levels of cyclin D1, protein levels decrease in 5 week transgenic liver and then increase in 8 week and 15 week transgenic liver (Fig. 4A). By 15 weeks, the transgenic liver are hyperplastic but do not contain definitive tumor nodules. Cyclin D1 protein levels are increased at least 4 fold above 15 week liver in tumors 1250/2-3, 1053/2-3 and 742/3-3 (Fig. 4A). The analysis demonstrated that 6/18 liver tumors overexpress cyclin D1 to levels 4 fold or above relative to 15 week liver (Table 1). Overexpression of cyclin D1 has previously been observed in 13% of human HCC which had DNA amplification of the *CCND1* gene (31).

Cyclin D1 overexpression does not frequently occur in tumors with cyclin A2 overexpression. A total of 3/18 tumors show overexpression of both cyclin A2 and cyclin D1. Thus, while cyclin D1 is overexpressed in some tumors, these results are not consistent with a generalized overexpression of cyclins in MTD2BL/6 liver tumors.

The proportion of cells within a liver tumor in S-phase was determined to clarify whether cyclin A2

overexpression is a consequence of a tumor-specific selective event or merely the result of many cells within a tumor progressing through the cell cycle. Cells that are not cycling are usually arrested in the G1-phase of the cell cycle (29). Histone *H3-2* RNA is expressed exclusively during S-phase and was therefore used as a direct measure of the proportion of cells within a tumor in S-phase (32) and as an indirect indicator of cell cycling within a tumor. As expected, normal adult liver express low levels of *H3-2* RNA (Fig. 4B). One week liver is a tissue that is actively cycling and thus expresses high levels of *H3-2* RNA (Fig. 4B). Whereas 5 week liver expresses lower levels of *H3-2*, 8 week liver expresses moderate amounts of *H3-2* RNA and reaches maximal levels by 15 weeks when the liver is hyperplastic (Fig. 4B). Histone *H3-2* levels in liver tumor samples are similar or somewhat less than levels observed in both 1 week and 15 week transgenic liver and do not appear to correlate with either cyclin A2 protein or cyclin D1 protein levels (Fig. 4B). That is, tumors with high cyclin A2 levels are not necessarily tumors with a high proportion of cells in S-phase. For example, tumors 1053/2-2,-3 express high levels of cyclin A2 and have high histone *H3-2* expression, while tumors 742/3-2,-3 also have high cyclin A2 level without high levels of histone *H3-2* (Figs. 4A and 4B). Of the 9 tumors that overexpress cyclin A2 (Table 1), 5 show levels of *H3-2* expression similar to or above 15 week transgenic liver. Conversely, 4/9 cyclin A2 overexpressing tumors have histone *H3-2* levels at least one half of levels observed in 15 week transgenic liver. This suggests that cyclin A2 overexpression is not simply a consequence of increased cell cycling, but may have some other role in tumor progression.

DISCUSSION

RLGS and the candidate gene approach were combined to define a tumor-specific amplification in liver tumors generated in SV40 TAG transgenic mice. RLGS analysis revealed one tumor with 6 spots amplified to similar levels, which is consistent with a contiguous amplicon. Two of these spots have previously been mapped (14), enabling us to further define the amplicon and analyze the expression of specific candidate oncogenes that were amplified in this chromosomal region. Whereas *Fgf2* expression is below the limit of detection in tumors, *CcnA2* RNA and cyclin A2 protein are both overexpressed in 4/18 and 9/18 liver tumors, respectively (Table 1). Additionally, a second tumor was found to have an amplification of the *CcnA2* gene. Taken together, these results are consistent with selection for the overexpression of *CcnA2* in a subset of tumors and exclude *Fgf2* as the gene driving selection for DNA amplification.

The studies presented here cannot unambiguously exclude the possibility that an unknown oncogene is

driving selection for the amplicon on proximal chromosome three. There are three lines of evidence however, that are consistent with cyclin A2 overexpression as a selective event in tumors. First, two tumors had a DNA amplification which included *CcnA2* and amplification events in tumors are uniquely selective. Additionally, *CcnA2* amplification was consistent with a large increase in RNA expression. Second, *CcnA2* RNA overexpression was found in tumors without DNA amplification. Third, cyclin A2 protein is overexpressed in many liver tumors to levels which are frequently far in excess of protein levels observed in actively growing tissues. Taken together, these points strongly suggest that cyclin A2 overexpression is a selective event during MTD2BL/6 tumorigenesis.

The selective advantage of cyclin A2 overexpression in MTD2BL/6 tumorigenesis can be inferred from the analysis of histone H3-2 expression. Histone H3-2 is expressed exclusively during S-phase of the cell cycle (32). Of the 9 tumors that show overexpression of cyclin A2 (Table 1), five exhibit levels of histone H3-2 equal to or above those observed in 15 week hyperplastic liver. Given that cyclin A2 is required during S-phase (33, 34), these results are consistent with overexpression having the expected positive effect on the cell cycle, presumably through the increased phosphorylation of its normal substrates. As well, cyclin A2 overexpression may promote cell cycling by persistence into the G1-phase where it is not normally expressed (35) and result in deregulated progression through the G1-to-S-phase transition (34). Alternatively, cyclin A2 overexpression may be permissive for cell cycling, but is unable to affect cell cycle kinetics in some tumors. Furthermore, since cyclin A2 protein overexpression does not always correlate with an increased proportion of S-phase cells within tumors, this indicates that increased cyclin A2 overexpression is not the simple consequence of cell cycling and may have some other role in tumorigenesis.

The overexpression of cyclin A2 has been observed in several human cancer cell lines (35, 36) and human tumor types (37, 38), including HCC (21, 39). Specifically, 12/31 (39%) human HCC samples exhibited cyclin A overexpression (21) and this frequency is similar to the 50% overexpression observed in MTD2BL/6 liver tumors (Table 1). In one particular HCC, an Hepatitis B Virus integration occurred in the *CCNA2* gene generating a mutant *CCNA2* transcript which was overexpressed (22). In addition, the mutant protein product translated from this RNA was found to be resistant to ubiquitin-mediated degradation (23) and was subsequently shown to be transforming (40).

Cyclin D1 protein levels were measured to exclude the possibility that liver tumors exhibited a generalized overexpression of cyclins. The results indicate that cyclin D1 is overexpressed in 6/18 tumors, of which three had cyclin A2 overexpression. This indicates that

a generalized overexpression of cyclins is unable to explain the overexpression of cyclin A2. Since cyclin D1 is expressed during G1-phase (29, 30), overexpression may result in persistence of cyclin D1 protein into other phases of the cell cycle. In human HCC, cyclin D1 is overexpressed in response to amplification of the *CCND1* gene in 11 to 13% of tumors analyzed (31, 41). The tumors in our study were not investigated for *CcnD1* amplification.

Thus, we have used RLGS and the candidate gene approach to define a tumor-specific amplification that occurs in MTD2BL/6 liver tumors. Our results indicate that the cyclin A2 gene is the likely target of this amplification event. Combined with our other analysis (1–6), the results indicate that our SV40 Tag induced liver tumor models accurately recapitulate genetic events that occur in human Hepatocellular carcinomas.

ACKNOWLEDGMENTS

We thank C. Rogler for gifts of plasmids, S. Weinreich and M. Ellsworth for technical assistance, W. Burhans, A. Kinneburgh, and C. Wenner for critical review of the manuscript, and R. Elliott for assistance with genetic distance calculations. This research was supported by NCI grant CA68612-03A1 awarded to W.A.H. and NCI Core Center Grant CA16056 awarded to Roswell Park Cancer Institute. C.P. was supported by NCI Grant CA16058.

REFERENCES

- Schirmacher, P., Held, W. A., Yang, D., Chisari, F. V., Rustum, Y., and Rogler, C. E. (1992) Reactivation of insulin-like growth factor II during hepatocarcinogenesis in transgenic mice suggests a role in malignant growth. *Cancer Res.* **52**, 2549–2556.
- Held, W. A., Pazik, J., O'Brien, J. G., Kerns, K., Gobey, M., Meis, R., Kenny, L., and Rustum, Y. (1994) Genetic analysis of liver tumorigenesis in SV40 T antigen transgenic mice implies a role for imprinted genes. *Cancer Res.* **54**, 6489–6495.
- Held, W. A., Mullins, J. J., Kuhn, N. J., Gallagher, J. F., Gu, G. D., and Gross, K. W. (1989) T antigen expression and tumorigenesis in transgenic mice containing a mouse major urinary protein/SV40 T antigen hybrid gene. *EMBO J.* **8**, 183–191.
- Haddad, R., and Held, W. A. (1997) Genomic imprinting and Igf2 influence liver tumorigenesis and loss of heterozygosity in SV40 T antigen transgenic mice. *Cancer Res.* **57**, 4615–4623.
- Ohsumi, T., Okazaki, Y., Okuizumi, H., Shibata, K., Hanami, T., Mizuno, Y., Takahara, T., Sasaki, N., Ueda, M., Muramatsu, M., *et al.* (1995) Loss of heterozygosity in chromosomes 1, 5, 7 and 13 in mouse hepatoma detected by systematic genome-wide scanning using RLGS genetic map. *Biochem. Biophys. Res. Commun.* **212**, 632–639.
- Akama, T. O., Okazaki, Y., Ito, M., Okuizumi, H., Konno, H., Muramatsu, M., Plass, C., Held, W. A., and Hayashizaki, Y. (1997) Restriction landmark genomic scanning (RLGS-M)-based genome-wide scanning of mouse liver tumors for alterations in DNA methylation status. *Cancer Res.* **57**, 3294–3299.
- Schirmacher, P., Held, W. A., Yang, D., Biempica, L., and Rogler, C. E. (1991) Selective amplification of periportal transitional cells precedes formation of hepatocellular carcinoma in SV40 large tag transgenic mice. *Am. J. Pathol.* **139**, 231–241.
- Okazaki, Y., Okuizumi, H., Sasaki, N., Ohsumi, T., Kuromitsu, J., Kataoka, H., Muramatsu, M., Iwade, A., Hirota, N., Kita-

- jima, M., *et al.* (1994) A genetic linkage map of the mouse using an expanded production system of restriction landmark genomic scanning (RLGS Ver. 1.8). *Biochem. Biophys. Res. Commun.* **205**, 1922–1929.
9. Hatada, I., Hayashizaki, Y., Hirotsune, S., Komatsubara, H., and Mukai, T. (1991) A genomic scanning method for higher organisms using restriction sites as landmarks. *Proc. Natl. Acad. Sci. USA* **88**, 9523–9527.
10. Costello, J. F., Fruhwald, M. C., Smiraglia, D. J., Rush, L. J., Robertson, G. P., Gao, X., Wright, F. A., Feramisco, J. D., Pelto-maki, P., Lang, J. C., Schuller, D. E., Yu, L., Bloomfield, C. D., Caligiuri, M. A., Yates, A., Nishikawa, R., Su Huang, H., Petrelli, N. J., Zhang, X., O'Dorisio, M. S., Held, W. A., Cavennee, W. K., and Plass, C. (2000) Aberrant CpG-island methylation has non-random and tumour-type-specific patterns [see comments]. *Nat. Genet.* **24**, 132–138.
11. Hughes, S. J., Glover, T. W., Zhu, X. X., Kuick, R., Thoraval, D., Orringer, M. B., Beer, D. G., and Hanash, S. (1998) A novel amplicon at 8p22–23 results in overexpression of cathepsin B in esophageal adenocarcinoma. *Proc. Natl. Acad. Sci. USA* **95**, 12410–12415.
12. Costello, J. F., Plass, C., Arap, W., Chapman, V. M., Held, W. A., Berger, M. S., Su Huang, H. J., and Cavennee, W. K. (1997) Cyclin-dependent kinase 6 (CDK6) amplification in human gliomas identified using two-dimensional separation of genomic DNA. *Cancer Res.* **57**, 1250–1254.
13. Komatsu, S., Okazaki, Y., Tatenno, M., Kawai, J., Konno, H., Kusakabe, M., Yoshiki, A., Muramatsu, M., Held, W. A., and Hayashizaki, Y. (2000) Methylation and downregulated expression of mac25/insulin-like growth factor binding protein-7 is associated with liver tumorigenesis in SV40T/t antigen transgenic mice, screened by restriction landmark genomic scanning for methylation (RLGS-M). *Biochem. Biophys. Res. Commun.* **267**, 109–117.
14. Hayashizaki, Y., Hirotsune, S., Okazaki, Y., Shibata, H., Aka-sako, A., Muramatsu, M., Kawai, J., Hirasawa, T., Watanabe, S., Shiroishi, T., *et al.* (1994) A genetic linkage map of the mouse using restriction landmark genomic scanning (RLGS). *Genetics* **138**, 1207–1238.
15. Gallagher, S. R., and Smith, J. A. (1994) One-dimensional gel electrophoresis of protein. In *Current Protocols in Molecular Biology* (F. A. Ausubel, R. Brent, R. E. Kingston, D. D. Moore, J. G. Seidman, J. A. Smith, and K. Struhl, Eds.), 10.2.1–10.2.18, John Wiley & Sons, New York.
16. Winston, S. E., Fuller, S. A., and Hurrell, J. G. (1994) Western blotting. In *Current Protocols in Molecular Biology* (F. A. Ausubel, R. Brent, R. E. Kingston, D. D. Moore, J. G. Seidman, J. A. Smith, and K. Struhl, Eds.), John Wiley & Sons, New York.
17. (1998) Mouse Genome Database (MGD), Vol. 1998 The Jackson Laboratory, Bar Harbor, Maine.
18. Manly, K. F. (1993) A Macintosh program for storage and analysis of experimental genetic mapping data. *Mamm. Genome* **4**, 303–313.
19. Otsuka, T., Takayama, H., Sharp, R., Celli, G., LaRochelle, W. J., Bottaro, D. P., Ellmore, N., Vieira, W., Owens, J. W., Anver, M., and Merlino, G. (1998) c-Met autocrine activation induces development of malignant melanoma and acquisition of the meta-static phenotype. *Cancer Res.* **58**, 5157–5167.
20. Kurokawa, M., Mitani, K., Irie, K., Matsuyama, T., Takahashi, T., Chiba, S., Yazaki, Y., Matsumoto, K., and Hirai, H. (1998) The oncoprotein Evi-1 represses TGF-beta signaling by inhibiting Smad3. *Nature* **394**, 92–96.
21. Chao, Y., Shih, Y. L., Chiu, J. H., Chau, G. Y., Lui, W. Y., Yang, W. K., Lee, S. D., and Huang, T. S. (1998) Overexpression of cyclin A but not Skp 2 correlates with the tumor relapse of human hepatocellular carcinoma. *Cancer Res.* **58**, 985–990.
22. Wang, J., Chenivresse, X., Henglein, B., and Brechot, C. (1990) Hepatitis B virus integration in a cyclin A gene in a hepatocellular carcinoma. *Nature* **343**, 555–557.
23. Wang, J., Zindy, F., Chenivresse, X., Lamas, E., Henglein, B., and Brechot, C. (1992) Modification of cyclin A expression by hepatitis B virus DNA integration in a hepatocellular carcinoma. *Oncogene* **7**, 1653–1656.
24. Abraham, J. A., Mergia, A., Whang, J. L., Tumolo, A., Friedman, J., Hjerrild, K. A., Gospodarowicz, D., and Fiddes, J. C. (1986) Nucleotide sequence of a bovine clone encoding the angiogenic protein, basic fibroblast growth factor. *Science* **233**, 545–548.
25. Mummery, C. L., van Rooyen, M., Bracke, M., van den Eijnden-van Raaij, J., van Zoelen, E. J., and Alitalo, K. (1993) Fibroblast growth factor-mediated growth regulation and receptor expression in embryonal carcinoma and embryonic stem cells and human germ cell tumours. *Biochem. Biophys. Res. Commun.* **191**, 188–195.
26. Nanus, D. M., Schmitz-Drager, B. J., Motzer, R. J., Lee, A. C., Vlamis, V., Cordon-Cardo, C., Albino, A. P., and Reuter, V. E. (1993) Expression of basic fibroblast growth factor in primary human renal tumors: Correlation with poor survival. *J. Natl. Cancer Inst.* **85**, 1597–1599.
27. Denny, P., Lord, C. J., Hill, N. J., Goy, J. V., Levy, E. R., Podolin, P. L., Peterson, L. B., Wicker, L. S., Todd, J. A., and Lyons, P. A. (1997) Mapping of the IDDM locus Idd3 to a 0.35-cM interval containing the interleukin-2 gene. *Diabetes* **46**, 695–700.
28. Porras, A., Bennett, J., Howe, A., Tokos, K., Bouck, N., Henglein, B., Sathiyamangalam, S., Thimmapaya, B., and Rundell, K. (1996) A novel simian virus 40 early-region domain mediates transactivation of the cyclin A promoter by small-t antigen and is required for transformation in small-t antigen-dependent assays. *J. Virol.* **70**, 6902–6908.
29. Morgan, D. O. (1997) Cyclin-dependent kinases: Engines, clocks, and microprocessors. *Annu. Rev. Cell Dev. Biol.* **13**, 261–291.
30. Sgambato, A., Flamini, G., Cittadini, A., and Weinstein, I. B. (1998) Abnormalities in cell cycle control in cancer and their clinical implications. *Tumori* **84**, 421–433.
31. Zhang, Y. J., Jiang, W., Chen, C. J., Lee, C. S., Kahn, S. M., Santella, R. M., and Weinstein, I. B. (1993) Amplification and overexpression of cyclin D1 in human hepatocellular carcinoma. *Biochem. Biophys. Res. Commun.* **196**, 1010–1016.
32. Alterman, R. B., Ganguly, S., Schulze, D. H., Marzluff, W. F., Schildkraut, C. L., and Skoultschi, A. I. (1984) Cell cycle regulation of mouse H3 histone mRNA metabolism. *Mol. Cell Biol.* **4**, 123–32.
33. Pagano, M., Pepperkok, R., Verde, F., Ansorge, W., and Draetta, G. (1992) Cyclin A is required at two points in the human cell cycle. *EMBO J.* **11**, 961–971.
34. Resnitzky, D., Hengst, L., and Reed, S. I. (1995) Cyclin A-associated kinase activity is rate limiting for entrance into S phase and is negatively regulated in G1 by p27Kip1. *Mol. Cell Biol.* **15**, 4347–4352.
35. Keyomarsi, K., and Pardee, A. B. (1993) Redundant cyclin over-expression and gene amplification in breast cancer cells. *Proc. Natl. Acad. Sci. USA* **90**, 1112–1116.
36. Buckley, M. F., Sweeney, K. J., Hamilton, J. A., Sini, R. L., Manning, D. L., Nicholson, R. I., deFazio, A., Watts, C. K., Musgrove, E. A., and Sutherland, R. L. (1993) Expression and amplification of cyclin genes in human breast cancer. *Oncogene* **8**, 2127–2133.
37. Dutta, A., Chandra, R., Leiter, L. M., and Lester, S. (1995) Cyclins as markers of tumor proliferation: Immunocytochemical studies in breast cancer. *Proc. Natl. Acad. Sci. USA* **92**, 5386–5390.
38. Volm, M., Koomagi, R., Mattern, J., and Stammers, G. (1997)

- Cyclin A is associated with an unfavourable outcome in patients with non-small-cell lung carcinomas. *Br. J. Cancer* **75**, 1774–1778.
39. Paterlini, P., Flejou, J. F., De Mitri, M. S., Pisi, E., Franco, D., and Brechot, C. (1995) Structure and expression of the cyclin A gene in human primary liver cancer. Correlation with flow cytometric parameters. *J. Hepatol.* **23**, 47–52.
40. Berasain, C., Patil, D., Perara, E., Huang, S. M., Mouly, H., and Brechot, C. (1998) Oncogenic activation of a human cyclin A2 targeted to the endoplasmic reticulum upon hepatitis B virus genome insertion. *Oncogene* **16**, 1277–1288.
41. Nishida, N., Fukuda, Y., Komeda, T., Kita, R., Sando, T., Furukawa, M., Amenomori, M., Shibagaki, I., Nakao, K., Ikenaga, M., *et al.* (1994) Amplification and overexpression of the cyclin D1 gene in aggressive human hepatocellular carcinoma. *Cancer Res.* **54**, 3107–3110.